ISSN 1070-3632, Russian Journal of General Chemistry, 2014, Vol. 84, No. 1, pp. 9–15. © Pleiades Publishing, Ltd., 2014.
Original Russian Text © V.V. Turovtsev, M.Yu. Orlov, R.V. Turovtsev, Yu.D. Orlov, 2014, published in Zhurnal Obshchei Khimii, 2014, Vol. 84, No. 1, pp. 11–17.

Internal Rotation in Mononitro-*n*-alkyl Radicals

V. V. Turovtsev[a,b], M. Yu. Orlov[b], R. V. Turovtsev[b], and Yu. D. Orlov[b]

[a] *Tver State Medical Academy, Tver, Russia*

[b] *Tver State University, ul. Zhelyabova 33, Tver, 170100 Russia*
e-mail: turtsma@tversu.ru

Received February 21, 2013

Abstract—Internal rotation in the $C^{\cdot}H_2(CH_2)_nNO_2$ ($n \le 7$) type radicals has been studied. 44 potential functions of the internal rotation, $V(\varphi)$, have been calculated taking advantage of the B3LYP/6-311++(3df,3pd) and MP2/6-311++(3df,3pd) methods. The trends observed in the series of parameters characterizing the internal rotation have been explained in view of the electron clouds conjugation, the inductive effect of the end groups, the gauche effect, and the rotation tops interaction. The coefficients of $V(\varphi)$ have been shown to depend predominantly on the nearest surrounding of the rotation axis. Based on this, the generalized functions, $V_{av}(\varphi)$, have been developed, their coefficients being dependent exclusively on the rotating bond position. Such functions are convenient for molecular modeling applications.

DOI: 10.1134/S1070363214010034

The electronic structure of mononitro-*n*-alkyl radicals $C^{\cdot}H_2(CH_2)_nNO_2$ is of special interest: the electron density $\rho(r)$ of their end group comprises two diffuse clouds, that of the unpaired electron of $C^{\cdot}H_2$ and that of lone-electron pairs of NO_2. The interaction (conjugation) of that clouds leads to substantial change of the $\rho(r)$ distribution as compared with the corresponding mononitro-*n*-alkanes, *n*-alkanes, and *n*-alkyl radicals. It should influence the potential functions of the internal rotation $V(\varphi)$ as well. The corresponding $V(\varphi)$ functions in the cases of alkanes, alkyl radicals, and mononitro-*n*-alkanes have been studied in detail in our previous reports [1–4]. It was demonstrated that the presence of the radical center $C^{\cdot}H_2$ significantly influenced the $V(\varphi)$ parameters of *n*-alkyl radicals and the energy barriers of rotation around the two adjacent C–C bonds. It was therefore of interest to study the similar changes in the heteroatom-containing radicals $C^{\cdot}H_2(CH_2)_nNO_2$; in particular, the rotation of radical group, its interaction with the heteroatoms, and comparison of the revealed effects with those in the cases of *n*-alkanes and mononitro-*n*-alkanes [5, 6] were in the focus of our attention.

The potential functions $V(\varphi)$ of mononitro-*n*-*trans*-alkyl radicals (44 functions in total, see Tables 1–5) for all the internal rotations in the $C^{\cdot}H_2(CH_2)_nNO_2$ radicals (n = 0–7) were computed by means of the B3LYP/6-311++(3df,3pd) method, the MP2/6-311++(3df,3pd) method was applied for similar calculations in the cases of several simplest homologs. All the computations were performed with GAUSSIAN software [7] using the Cartesian basis 6d, 10f. The incremental step of the dihedral angle φ was of 10°. For each of the rotations, the location of the transition state and the local minimum along with the corresponding total energy values were refined. In particular, the transition states were found taking advantage of the QST3 procedure [8]. The inaccuracy of numerical calculation of the total energy E_{tot} was below 1×10^{-10} a. u. (less than 1 J/mol), and that of the matrix elements was below 3×10^{-6}. In view of that, the coefficients of the Fourier decompositions of $V(\varphi)$ (Tables 1–5) were given with the accuracy of 1 J/mol. The $V(\varphi)$ functions corresponding to rotation around C–N bonds were approximated with the series (1) with n = 2, whereas those corresponding to rotation around C–C bonds were approximated with Eq. (1) (n = 1) and Eq. (2); the quality of all the approximations were evaluated by calculating the residual Δ [2, 3].

$$V(\varphi) = \sum_{m=1}^{6} \frac{V_{mn}}{2} [1 - \cos(mn\varphi)], \quad (1)$$

$$V(\varphi) = V_0 + \sum_{m=1}^{6} V_m \cos(m\varphi). \quad (2)$$

Table 1. Coefficients of series (1) in the case of (C)–NO_2 top rotation (kJ/mol)

Molecule	V_2	V_4	V_6	V_8	V_{10}	V_{12}	Δ	V_{glob}	V_{min}
CH_2–NO_2 (MP2)	20.26	–4.898	1.8506	–0.858	–0.143	0.625	1.096	22.66	–
C_2H_4–NO_2 (MP2)	1.044	0.257	–0.115	0.032	0.001	–0.008	0.002	1.03	0.93
C_3H_6–NO_2 (MP2)	3.735	0.481	–0.228	–0.059	0.003	–0.002	0.138	3.51	–
CH_2–NO_2	24.523	–5.835	1.493	–0.986	0.661	–0.466	0.216	29.07	–
C_2H_4–NO_2	0.459	0.306	–0.013	0.031	–0.002	0.011	0.003	0.60	0.44
C_3H_6–NO_2	1.737	–0.062	–0.140	0.029	0.015	0.001	0.008	1.62	–
C_4H_8–NO_2	1.735	0.224	–0.063	–0.017	–0.024	0.000	0.079	1.66	–
C_5H_{10}–NO_2	1.646	0.217	–0.100	0.002	–0.008	–0.002	0.093	1.57	–
C_6H_{12}–NO_2	1.856	0.261	–0.126	–0.034	–0.017	–0.001	0.056	1.76	–
C_7H_{14}–NO_2	1.924	0.283	–0.102	–0.014	–0.001	0.024	0.065	1.90	–
C_8H_{16}–NO_2	2.048	0.241	–0.151	0.119	–0.038	0.032	0.040	2.03	1.85
V_{av}	1.824	0.194	–0.114	0.014	–0.012	0.009	–	1.76	–

Table 2. Coefficients of series (1) in the case of C_2H_4–(C) top rotation (kJ/mol)

Molecule	V_1	V_2	V_3	V_4	V_5	V_6	Δ	V_{glob}	V_{loc}	V_{min}	$V_{trans\text{-}gouche}$	V_{gauche}
C_2H_4–CH_2NO_2	7.187	–4.975	13.551	–0.367	–0.399	–0.128	0.089	20.25	11.28	0.66	10.62	19.59
C_2H_4–$C_2H_4NO_2$	5.987	–4.966	14.588	–0.090	–0.411	–0.105	0.232	20.10	12.24	0.0	12.24	12.24
C_2H_4–$C_3H_6NO_2$	7.953	–5.087	14.255	–0.132	–0.682	–0.306	0.125	21.32	12.27	0.96	11.31	20.36
C_2H_4–$C_4H_8NO_2$	7.983	–5.429	14.082	–0.139	–0.595	–0.214	0.116	21.29	11.90	0.76	11.14	20.54
C_2H_4–$C_5H_{10}NO_2$	8.718	–5.945	14.021	0.571	–0.659	–0.091	0.141	21.64	12.17	1.17	10.99	20.46
C_2H_4–$C_6H_{12}NO_2$	8.807	–6.157	13.835	0.693	–0.668	0.050	0.124	21.53	11.86	1.18	10.68	20.35
V_{av}	8.130	–5.519	13.949	0.125	–0.601	–0.138	–	21.20	11.89	0.95	10.95	20.26

$C^{\cdot}H_2NO_2$ radical, the simplest one within the studied series, was planar as concluded from the B3LYP/6-311++(3df,3pd) and MP2/6-311++(3df,3pd) results, being of the C_{2V} point group. The close location of $C^{\cdot}H_2$ and NO_2 groups in that compound led to strong interaction of the end groups electron clouds (their conjugation) reflected in the fairly high energy barrier V_{glob}, of 29.07 kJ/mol (B3LYP) and 22.66 kJ/mol (MP2) (Table 1 and Fig. 1). Noteworthily, in the case of the parent compound with the closed electron shell (CH_3NO_2), the respective V_{glob} value as calculated with the MP2 method (0.05 kJ/mol) was higher than that calculated using the B3LYP approach (0.03 kJ/mol), whereas result was the opposite in the case of radical $C^{\cdot}H_2NO_2$. The increase of the barrier value in the case of $C^{\cdot}H_2NO_2$ was explained by the "stabilizing conjugation:" in the case of CH_3–NO_2, the V_{glob} was 2.5 orders of magnitude lower [4]. Similarly, in the case of $^{\cdot}CH_2$–CH_3, the end groups inductive effects without conjugation led to relatively low V_{glob}, of 0.23 kJ/mol [1]. The approximation of $C^{\cdot}H_2NO_2$ potential energy surface with the (1) series was poorly convergent in the case of the MP2/6-311++(3df,3pd) method, as revealed by quite significant residual Δ ~ 1 kJ/mol (the residual was 5 times lower in the case of the B3LYP method). The $V(\varphi)$ coefficients in the both decompositions were significant (Table 1), reflecting the substantial rearrangement of $\rho(r)$ with the altering dihedral angle φ (Fig. 1).

In terms of quantum chemistry, the increase of rotation energy barrier due to conjugation could be represented as spreading of the unpaired electron density $\rho_e(r)$ towards the neighboring groups (in the

Table 3. Coefficients of series (1) in the case of rotation around the (C)–C–C–(C) bond (kJ/mol)

Molecule	V_1	V_2	V_3	V_4	V_5	V_6	Δ	V_{glob}	V_{loc}	V_{min}	$V_{trans\text{-}gouche}$	V_{gauche}
C_3H_6–$C_2H_4NO_2$	9.915	–4.590	13.119	–0.752	0.438	–0.455	0.030	23.50	11.74	3.42	8.32	20.08
C_4H_8–$C_2H_4NO_2$	9.448	–4.128	13.112	–0.619	0.395	–0.445	0.020	22.98	12.03	3.47	8.56	19.51
C_3H_6–$C_3H_6NO_2$	9.811	–4.542	13.416	–0.656	0.387	–0.416	0.035	23.72	12.10	3.40	8.71	20.32
C_5H_{10}–$C_2H_4NO_2$	9.492	–4.130	13.152	–0.711	0.405	–0.495	0.029	23.12	11.98	3.47	8.50	19.65
C_3H_6–$C_4H_8NO_2$	10.348	–4.649	13.287	–0.763	0.361	–0.431	0.030	24.06	11.97	3.59	8.38	20.47
C_3H_6–$C_5H_{10}NO_2$	10.154	–4.618	13.374	–0.746	0.370	–0.470	0.020	23.93	11.99	3.54	8.45	20.39
C_4H_8–$C_3H_6NO_2$	9.787	–4.407	13.432	–0.630	0.335	–0.433	0.026	23.64	12.19	3.50	8.69	20.14
C_4H_8–$C_4H_8NO_2$	9.979	–4.501	13.319	–0.588	0.372	–0.398	0.032	23.73	12.08	3.65	8.43	20.08
C_5H_{10}–$C_3H_6NO_2$	9.517	–4.268	13.360	–0.683	0.459	–0.485	0.042	23.39	12.22	3.51	8.71	19.89
C_6H_{12}–$C_2H_4NO_2$	9.356	–4.162	13.199	–0.651	0.401	–0.478	0.042	23.01	12.01	3.52	8.49	19.49
V_{av}	9.781	–4.400	13.277	–0.680	0.392	–0.451	–	23.51	12.03	3.51	8.52	20.00

Table 4. Coefficients of series (2) in the cases of top rotation around the (C)–CH_2NO_2 and (C)–$C_2H_4NO_2$ bonds (kJ/mol)

Molecule	V_0	V_1	V_2	V_3	V_4	V_5	V_6	Δ	V_{glob}	V_{loc}	V_{min}	$V_{trans\text{-}gouche}$
C_2H_4–CH_2NO_2 (MP2)	8.934	–0.928	1.180	–8.409	0.492	0.319	0.027	0.226	19.69	15.95	–1.69	1.69
C_2H_4–CH_2NO_2	7.426	–3.612	2.470	–6.795	0.165	0.181	0.047	0.082	20.25	11.28	0.66	10.62
C_3H_6–CH_2NO_2	7.015	–2.712	2.605	–6.619	0.239	0.071	0.005	0.028	19.15	10.93	–0.62[a]	10.93
C_2H_4–$C_2H_4NO_2$	7.550	–2.886	2.587	–7.184	0.149	0.314	0.150	0.116	20.10	12.24	–0.60[a]	12.24
C_4H_8–CH_2NO_2	7.013	–2.849	2.480	–6.843	0.203	0.020	–0.008	0.019	19.36	11.10	0.00	11.10
C_5H_{10}–CH_2NO_2	7.056	–2.624	2.345	–6.858	0.200	0.019	–0.024	0.022	18.99	11.32	0.00	11.32
C_6H_{12}–CH_2NO_2	7.025	–2.718	2.344	–6.855	0.219	0.006	–0.007	0.022	19.18	11.21	–0.036[a]	11.21
C_7H_{14}–CH_2NO_2	6.976	–2.671	2.330	–6.865	0.187	0.044	0.016	0.026	19.01	11.32	0.00	11.21
V_{av}	7.106	–2.743	2.449	–6.871	0.199	0.079	0.022	–	19.30	11.35	0.00	11.34

[a] The total energy of *gauche* conformer is slightly lower than that of *trans* conformer.

considered case, NO_2), and vice versa. The interaction of nuclei with the electron density delocalized along several atoms enhanced the structure rigidity. Such interaction changed the overall electron density, not only its local parts $\rho_R(r)$ (R, a fragment isolated in terms of the electron density interaction); therefore, the nuclei motion was coordinated, and the energy barriers of internal rotation were enhanced (Fig. 1).

In the case of the next homolog ($C^{\cdot}H_2CH_2$–NO_2), the NO_2 rotation barrier (Table 1 and Fig. 2) was sharply decreased down to 0.60 kJ/mol (it was also fairly low in the case of the parent compound C_2H_5–NO_2, 0.37 kJ/mol [4]). Likely, that was due to the more localized unpaired electron at the radical center ($^{\cdot}CH_2$) and thus less perturbation of $\rho_{NO2}(r)$ caused by the radical. In the cases of other homologs, starting with $^{\cdot}C_3H_6NO_2$, the nitro group rotation was negligibly affected by the compound chain length (Table 1 and Fig. 2). With increasing the methylene chain length, the parameters related to the internal rotation in mononitro-*n*-alkyl radicals rapidly converged to the

Table 5. Coefficients of series (2) in the case of $C^{\cdot}H_2$–(C) top rotation (kJ/mol)

Molecule	V_0	V_1	V_2	V_3	V_4	V_5	V_6	Δ	V_{glob}	V_{loc}	V_{min}
CH_2–CH_2NO_2 (MP2)	0.821	0.034	–0.994	–0.013	0.385	–0.003	–0.269	0.255	2.88	–	–
CH_2–CH_2NO_2	1.226	–0.061	–1.218	0.049	0.194	–0.026	–0.194	0.061	2.96	–	–
CH_2–$C_2H_4NO_2$ (MP2)	0.548	0.011	–0.609	–0.012	0.194	0.011	–0.142	0.028	1.46	0.33	0.30
CH_2–$C_2H_4NO_2$	0.469	0.006	–0.616	–0.004	0.234	0.007	–0.094	0.010	1.42	–	–
CH_2–$C_3H_6NO_2$	0.292	0.016	–0.226	–0.028	0.086	–0.010	0.129	0.023	0.54	0.27	0.46
CH_2–$C_4H_8NO_2$	0.412	0.001	–0.385	0.001	0.093	0.001	0.122	0.034	0.80	0.27	–
CH_2–$C_5H_{10}NO_2$	0.412	–0.006	–0.425	0.022	0.071	0.024	0.120	0.022	0.82	0.20	0.80
CH_2–$C_6H_{12}NO_2$	0.451	0.025	–0.441	–0.013	0.074	–0.018	0.124	0.024	0.87	0.24	0.85
CH_2–$C_7H_{14}NO_2$	0.423	0.000	–0.438	0.000	0.051	0.000	0.117	0.057	0.84	0.21	0.82
V_{av}	0.410	0.007	–0.422	–0.004	0.101	0.001	0.086	–	0.88	0.24	0.73

corresponding values in the cases of *n*-alkanes, *n*-alkyl radicals [1–3], and mononitro-*n*-alkanes [4]. In particular, the parameters of NO_2 rotation in the studied radicals and the parent molecules were independent of the chain length starting from $CH_3(CH_2)_3$–NO_2 and from $C^{\cdot}H_2(CH_2)_5$–NO_2, respectively. In other words, the nitro group electron density was not much affected by the neighboring groups, and thus the $\rho_{NO2}(r)$ function could be referred to as closed (isolated). The same applied to the $C^{\cdot}H_2CH_2$– atoms group [1, 2]. Therefore, the derived properties of the fragments partial properties, including those related to rotation, could be transferred to the compounds of other classes.

Disturbance of the conjugation of the electron clouds of end groups did not prevent the end groups interaction completely; however, it was screened by the indifferent CH_2 fragments (Tables 2 and 3). The end groups interaction was reflected in the double *gauche*-effect [9] in $C^{\cdot}H_2(CH_2)_3NO_2$: the equality of the energies of *trans*- and *gauche*$^{\pm}$-conformers upon rotation around the $C^{\cdot}H_2CH_2$–$(CH_2)_2NO_2$ and

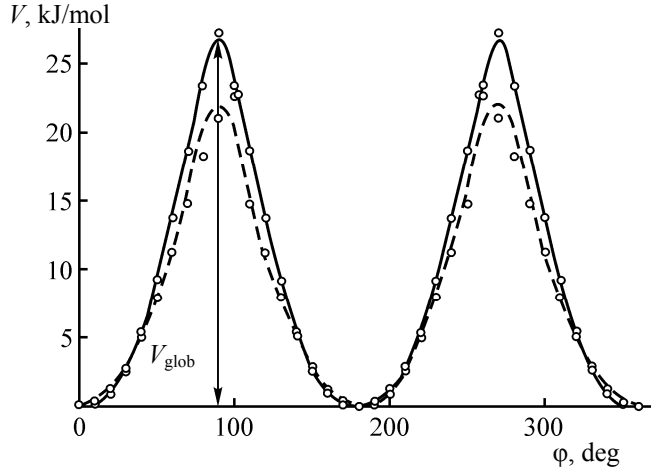

Fig. 1. Potential function $V(\varphi)$ of the internal rotation in $^{\cdot}CH_2$–NO_2. (Solid line) shows the B3LYP/6-311++(3df,3pd) result, (dashed) line shows the MP2/6-311++(3df,3pd) result.

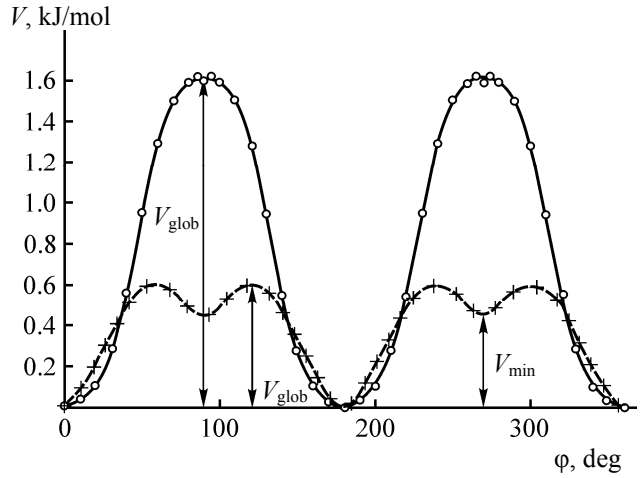

Fig. 2. Potential function $V(\varphi)$ of the NO_2 top rotation in the cases of $^{\cdot}C_2H_4$–NO_2 (crosses) and $^{\cdot}C_3H_6$–NO_2 (circles).

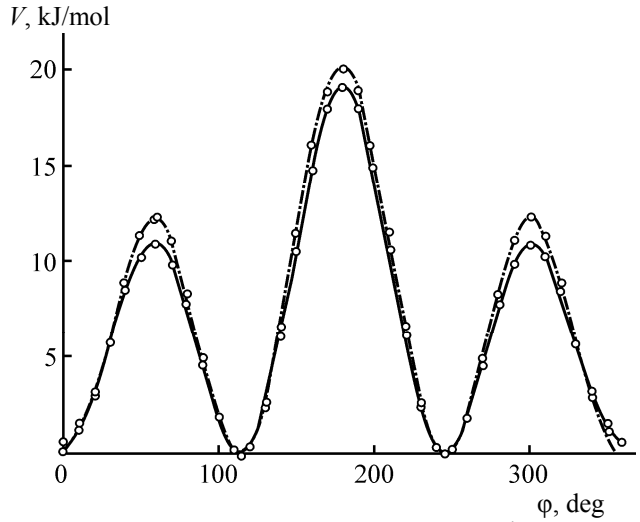

Fig. 3. The double *gauche* effect in the case of $\dot{C}_4H_8NO_2$: potential functions $V(\varphi)$ of rotation in the cases of $\dot{C}_2H_4$–$C_2H_4NO_2$ (dash-dot line) and $\dot{C}_3H_6$–CH_2NO_2 (solid line).

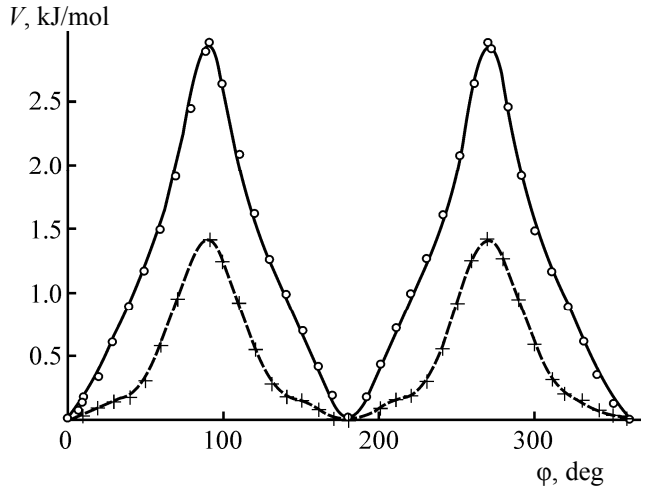

Fig. 4. Potential function $V(\varphi)$ of the $C\dot{H}_2$ top rotation in the case of $C\dot{H}_2$–CH_2NO_2 (circles) and $C\dot{H}_2$–$C_2H_4NO_2$ (crosses).

$C\dot{H}_2(CH_2)_2$–CH_2NO_2 bonds. Another consequence of the end groups interaction was the structural dissimilarity of $C\dot{H}_2(CH_2)_nNO_2$ ($n < 4$) and the higher homologs (the point group of the nuclei locations at $n < 4$ was C_S, changing to C_1 group at $n \geq 4$). The areas of operation of the $C\dot{H}_2$ and NO_2 inductive effects overlapped to some extend in the cases of all the studied radicals (Tables 1–5); however, starting from $n = 6$, the interference of $C\dot{H}_2$ and NO_2 effects could be neglected, and their motion could be examined independently. Hence, at $n \geq 6$, the barrier values and the coefficients of $V(\varphi)$ decompositions related to rotation within the $C\dot{H}_2CH_2(C)$, $(C)(CH_2)_n(C)$, and $(C)(CH_2)_4NO_2$ fragments were independent of the rest of the compound (Tables 2–4). It was reasonable to suggest that the change of a certain bond $V(\varphi)$ coefficients was directly related to the changes of the electron density in the bond nearest surrounding; hence, the inductive effect of $C\dot{H}_2$ and NO_2 determined the $V(\varphi)$ of the respective nearest bonds.

The rotation of molecular fragments led to certain rearrangements of other parts of the radicals. In some cases, that induced the consistent motion of the distant fragments, in other words, the rotation tops interacted with each other. In particular, rotation around the C–C bonds in $C\dot{H}_2CH_2$–$(CH_2)_nNO_2$ and $C\dot{H}_2(CH_2)_n$–CH_2NO_2, $n \geq 2$ (Tables 2–4) changed the locations of $C\dot{H}_2$ and NO_2 end groups with respect to the hydrocarbon chain (oscillations of the dihedral and bond angles as well as of the C–H, C–C, and C–N bond lengths), whereas the atoms motion in other fragments was negligible. The most efficient interaction of the rotation tops was observed in the cases of lower homologs $C\dot{H}_2CH_2NO_2$ and $C\dot{H}_2(CH)_2NO_2$: in those cases, rotation of $\dot{C}H_2$ induced rotation of hydrogen atoms in the hydrocarbon chain. Each of the studied internal rotations could be described be the one-dimensional $V(\varphi)$ function (the slice of potential energy surface). In order to describe the rotation tops interaction, the multi-dimensional projections of the potential energy surface should have been examined. In the classical case, the number of internal degrees of freedom equaled $3N - 6$ (N being the number of atoms) and corresponded to the number of independent internal nuclear motions; each motion corresponding to the certain set of energy levels. The level sets were located in the potential wells, formed in turn by the intramolecular field. The rotation tops interaction decreased the number of independent degrees of freedom by the number of consistent motions; simultaneously the number of multipliers of the internal statistical sum was decreased. Precise description of the above-mentioned phenomenon required using the three-dimensional potential functions $V(\varphi_1,\varphi_2,\varphi_3)$; in the cases of relatively long homologs, two-dimensional functions $V(\varphi_1,\varphi_2)$ were enough. Nevertheless, in thermodynamic calculations the assumption of the completely independent motions leading to the unidimensional slices $V(\varphi)$ gave satisfactory results.

In the cases of $C\dot{H}_2(CH_2)_nNO_2$ and $CH_3(CH_2)_nNO_2$ ($n \geq 2$), rotation around the (C)–CH_2NO_2 bond led to appearance of several conformers with the same total

energy (*gauche*-effect) [9] (Table 4). Therefore, the studied compounds consisted of the equilibrium mixture of the conformers. In contrast to the parent molecules with the closed electron shell, in the case of $C^{\cdot}H_2(CH_2)_3NO_2$, the double *gauche*-effect was observed: upon rotation around the $C^{\cdot}H_2(CH_2)_2$–CH_2NO_2 and $C^{\cdot}H_2CH_2$–$(CH_2)_2NO_2$ bonds, the conformational transition barriers being of 19.15 kJ/mol and 20.10 kJ/mol, respectively (Fig. 3 and Table 4). To some extent, the described features could be due to the symmetrical structure of the radical: the dovetail end groups (point symmetry group of C_S), and the electron density redistribution upon the rotation tops revealed similar behavior. The difference of the end groups chemical nature led, however, to the slightly different V_{glob} values and the $V(\varphi)$ coefficients.

The major electron density redistribution upon the fragments rotation occurred near the bond connecting the rotation tops. The more efficient was the interaction of the nuclei with the electron density, the higher were the barriers (as the electron density deformation required more energy); on the contrary, more diffuse electron density led to lower V_{glob}. The increase of the chain length from $C^{\cdot}H_2(CH_2)_3NO_2$ to $C^{\cdot}H_2(CH_2)_4NO_2$ disrupted the symmetrical distribution of the nuclei and the electron clouds, the nuclear symmetry was decreased to C_1 group, thus affecting the $V(\varphi)$ parameters: they became closer to those in the parent closed-shell molecules.

The electron density of the radical center $^{\cdot}CH_2$ was more diffuse than that of NO_2. The higher mobility of the unpaired electron density resulted in the lower $C^{\cdot}H_2$–(C) rotation barrier as compared to that of (C)–NO_2 in the cases of relatively long chains (Table 5). In particular, in the absence of conjugation, the V_{glob} value corresponding to the $C^{\cdot}H_2$ rotation was of 0.8 kJ/mol and that corresponding to NO_2 rotation was of 1.8 kJ/mol. The values of V_{glob} were somewhat different in the cases of lower homologs: $C^{\cdot}H_2$–CH_2NO_2 (2.96 kJ/mol), $C^{\cdot}H_2$–$C_2H_4NO_2$ (1.42 kJ/mol), and $C^{\cdot}H_2CH_2$–NO_2 (0.60 kJ/mol); the respective profiles of potential energy surfaces were different as well (Fig. 4).

The shortest methylene chain allowing to isolate the non-perturbed rotation of $C^{\cdot}H_2$ was found in $C^{\cdot}H_2(CH_2)_4NO_2$, and further increase of CH_2 groups number did not change the $V(\varphi)$ of $C^{\cdot}H_2$ rotation top. The parameters of $C^{\cdot}H_2$ internal rotation in $C^{\cdot}H_2$–$(CH_2)_nNO_2$ at $n \geq 4$ coincided with the respective values in the cases of *n*-alkyl radicals $C^{\cdot}H_2$–$(CH_2)_mCH_3$ at $m \geq 4$. Hence, at $n \geq 4$, any significant interaction of the electron clouds of $C^{\cdot}H_2$ and NO_2 vanished. In the cases of even longer chains, the rotation top around the C–C bond in $C^{\cdot}H_2(CH_2)_k$–$(CH_2)_mNO_2$ ($k \geq 2$ and $m \geq 6$) could be described by the $V(\varphi)$ functions practically identical to those in the cases of $C^{\cdot}H_2$–$(CH_2)_nCH_3$, $CH_3(CH_2)_nCH_3$, and $CH_3(CH_2)_nNO_2$. Thus, the perturbing effect of the radical center and of NO_2 was limited to the electron density of the nearest bonds; therefore, in the cases of long enough chains, the parameters of $V(\varphi)$ of the respective internal rotations could be extracted from the tabulated results related to $C^{\cdot}H_2(CH_2)_nCH_3$ [1, 2], $CH_3(CH_2)_nCH_3$ [3], or $CH_3(CH_2)_nNO_2$ [4], with no need for the resource-taking computations of the heteroatoms-containing radicals. Furthermore, in predicting the internal rotation properties, the $C^{\cdot}H_2(CH_2)_nNO_2$ radicals could be represented as combination of three parts: *n*-alkyl radical, *n*-alkane, and mononitro-*n*-alkane.

The additivity of the parameters of internal top rotation of the certain type (Tables 1–5) allowed elucidating the averaged parameters corresponding to each of the motion types, V_{av}. Such generalized parameters can be used in modeling the larger molecules with molecular mechanics and molecular dynamics methods, for instance, in computing their spectral and thermodynamic properties.

ACKNOWLEDGMENTS

This work was financially supported by the Federal Program “Scientific and Scientific-Pedagogical Personnel of Innovative Russia” for 2009–2013 (grant 14.B37.21.0835).

REFERENCES

1. Turovtsev, V.V. and Orlov, Yu.D., *Russ. J. Gen. Chem*., 2010, vol. 80, no. 4, p. 749.
2. Turovtsev, V.V. and Orlov, Yu.D., *Russ. J. Gen. Chem*., 2011, vol. 81, no. 9, p. 1798.
3. Turovtsev, V.V., Orlov, Yu.D., Kizin, A.N., and Lebedev, Yu.A., *Russ. J. Gen. Chem*., 2007, vol. 77, no. 9, p. 1580.
4. Turovtsev, V.V., Orlov, M.Yu., Turovtsev, R.V., and Orlov, Yu.D., *Russ. J. Phys. Chem., A,* 2012, vol. 86, no. 10, C. 1549.
5. Turovtsev, V.V., Orlov, Yu.D., and Lebedev, Yu.A., *Russ. J. Phys. Chem., A,* 2009, vol. 83, no. 2, p. 245.
6. Turovtsev, V.V., Orlov, M.Yu., Turovtsev, R.V., and

Orlov, Yu.D., *Russ. J. Phys. Chem., A,* 2012, vol. 86, no. 7, p. 1073.

7. Frisch, M.J., Trucks, G.W., Schlegel, H.B., Scuseria, G.E., Robb, M.A., Cheeseman, J.R., Scalmani, G., Barone, V., Mennucci, B., Petersson, G.A., Nakatsuji, H., Caricato, M., Li, X., Hratchian, H.P., Izmaylov, A.F., Bloino, J., Zheng, G., Sonnenberg, J.L., Hada, M., Ehara, M., Toyota, K., Fukuda, R., Hasegawa, J., Ishida, M., Nakajima, T., Honda, Y., Kitao, O., Nakai, H., Vreven, T., Montgomery, J.A., Jr., Peralta, J.E., Ogliaro, F., Bearpark, M., Heyd, J.J., Brothers, E., Kudin, K.N., Staroverov, V.N., Kobayashi, R., Normand, J., Raghavachari, K., Rendell, A., Burant, J.C., Iyengar, S.S., Tomasi, J., Cossi, M., Rega, N., Millam, J.M., Klene, M., Knox, J.E., Cross, J.B., Bakken, V., Adamo, C., Jaramillo, J., Gomperts, R., Stratmann, R.E., Yazyev, O., Austin, A.J., Cammi, R., Pomelli, C., Ochterski, J.W., Martin, R.L., Morokuma, K., Zakrzewski, V.G., Voth, G.A., Salvador, P., Dannenberg, J.J., Dapprich, S., Daniels, A.D., Farkas, O., Foresman, J.B., Ortiz, J.V., Cioslowski, J., and Fox, D.J., *GAUSSIAN 03* (Revision E 0.1), Gaussian Inc., Pittsburgh PA, 2007.
8. Peng, C., Ayala, P.Y., Schlegel, H.B., and Frisch, M.J., *J. Comp. Chem*., 1996, vol. 17, p. 49.
9. Wolfe, S., *Acc. Chem. Res*., 1972, vol. 5, no. 3, p. 102.